

# Novel mechanism for defective receptor binding of apolipoprotein E2 in type III hyperlipoproteinemia

Li-Ming Dong<sup>1</sup>, Sean Parkin<sup>3</sup>, Sergei D. Trakhanov<sup>1</sup>, Bernhard Rupp<sup>3</sup>, Trey Simmons<sup>1</sup>, Kay S. Arnold<sup>1</sup>, Yvonne M. Newhouse<sup>1</sup>, Thomas L. Innerarity<sup>1,2</sup> and Karl H. Weisgraber<sup>1</sup>

**The defective binding of apolipoprotein (apo) E2 to lipoprotein receptors, an underlying cause of type III hyperlipoproteinemia, results from replacement of Arg 158 with Cys, disrupting the naturally occurring salt bridge between Asp 154 and Arg 158. A new bond between Asp 154 and Arg 150 is formed, shifting Arg 150 out of the receptor binding region. Elimination of the 154–150 salt bridge by site-directed mutagenesis of Asp 154 to Ala restored the receptor binding activity to near normal levels. The X-ray crystal structure of apoE2 Ala 154 demonstrated that Arg 150 was relocated within the receptor binding region. Our results demonstrate that defective binding of apoE2 occurs by a novel mechanism of the replacement of one salt bridge with another.**

<sup>1</sup>The Gladstone Institute of Cardiovascular Disease and <sup>2</sup>Cardiovascular Research Institute, and Department of Pathology, University of California, P.O. Box 419100, San Francisco, California 94141-9100, USA  
<sup>3</sup>Biology and Biotechnology Research Program, Lawrence Livermore National Laboratory, Livermore, California 94550, USA

Correspondence should be addressed to K.H.W.

Human apolipoprotein (apo) E (299 amino acids), associated with several classes of plasma lipoproteins, participates in transporting cholesterol and triglycerides between tissues through its interaction with the low density lipoprotein (LDL) receptor and other lipoprotein receptors<sup>1,2</sup>. The three common isoforms differ at two polymorphic sites. Apolipoprotein E3 (Cys 112, Arg 158) and apoE4 (Arg 112, Arg 158) bind to the LDL receptor normally, whereas apoE2 (Cys 112, Cys 158) is defective in binding (0.1% of apoE3 or apoE4 activity)<sup>3,4</sup>. This binding defect results in delayed receptor-mediated clearance of lipoproteins from blood and, in combination with genetic, hormonal or environmental influences, results in familial type III hyperlipoproteinemia, a genetic disorder characterized by elevated plasma cholesterol and triglyceride levels and accelerated coronary artery disease<sup>5</sup>.

The defective binding of apoE2 to the LDL receptor is caused by the Arg to Cys substitution at position 158, which lies outside the receptor-binding region (residues 136–150)<sup>1,6–8</sup>. Because this substitution was outside the receptor binding region, its effect was suggested to occur by an

unknown indirect mechanism (that is, Arg 158 does not interact directly with the LDL receptor but in some way influences the residues that are located within the receptor binding region)<sup>9</sup>. This is in contrast to the direct disruption of receptor binding activity caused by the substitution of positively charged residues within the receptor binding region<sup>7</sup>. Because of the association of the defective receptor binding of apoE2 with type III hyperlipoproteinemia, it is important to understand how a single amino acid substitution may exert such a profound effect in an indirect manner. Here we report that the defective binding of apoE2 to the LDL receptor occurs by a novel molecular mechanism of disruption of a single salt bridge and formation of a new one.

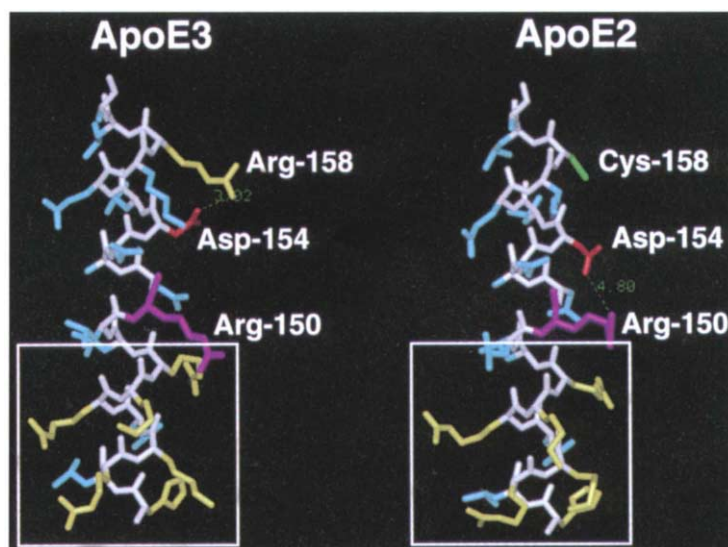


**Fig. 1** Stick representation of the  $\alpha$ -helical structures in the vicinity of the LDL receptor binding region of apoE3 and apoE2 (residues 140–160). The LDL receptor-binding region of apoE is indicated by the boxed area. Models were prepared using Insight II (Biosym).

**Table 1** Data collection statistics of apoE 22,000  $M_r$  fragments

Dataset	apoE3 (set 1)	apoE3(set 2)	apoE2 Ala 154
Resolution (Å)	8.0–1.8	8.0–1.8	8.0–2.0
No. reflections	16608	16667	12387
No. reflections ( $I > 2\sigma(I)$ )	11320	11170	8964
Redundancy	3.8	3.1	3.5
Completeness (%)	93.7	94.0	94.2
Completeness (%) ( $I > 2\sigma(I)$ )	63.9	63.0	72.0
$R_{\text{merge}}$ (%)	3.73	3.13	5.09

### Rearrangement of the Arg 150 side chain

Examination of the X-ray crystal structure of apoE2 22,000  $M_r$  fragment revealed that salt bridges were disrupted and rearranged in apoE2 with Cys at position 158 (ref. 10). The critical salt bridges are shown in Fig. 1. In apoE3, a salt bridge normally occurs between Arg 158 and Asp 154. In contrast, substitution of Cys for Arg 158, which distinguishes apoE2 from apoE3, eliminates the 154–158 salt bridge, and a new salt bridge is formed between Asp 154 and the previously unbridged Arg 150. As a consequence, the Arg 150 side chain is now repositioned out of the receptor binding region (residues 136–150). These results suggest that the formation of the new salt bridge may be responsible for the defective binding of apoE2.

### Recovery of normal receptor binding

Based on the suggestion from the apoE3 and apoE2 crystal structures that the 150–154 salt bridge may be a key determinant for the defective receptor binding of apoE2, we substituted Asp 154 with Ala in apoE2 (apoE2 Ala 154) by site-directed mutagenesis to eliminate the 150–154 salt bridge. The protein was produced in *Escherichia coli*, and the receptor binding activity of the mutant apoE2 was determined. As shown in Fig. 2, replacement of Asp 154 by Ala increased the receptor binding activity of apoE2 to near normal levels. The concentration of apoE2 Ala 154 required for 50% displacement of  $^{125}\text{I}$ -LDL in

the receptor binding assay was  $0.06 \pm 0.03 \mu\text{g ml}^{-1}$  ( $n=6$ ), compared with  $0.05 \pm 0.02 \mu\text{g ml}^{-1}$  ( $n=5$ ) for apoE3 or ~80% of normal binding activity.

### Repositioning of the Arg 150 side chain

The restoration of LDL receptor binding activity to near normal levels with the apoE2 Ala 154 mutant suggested that disruption of the 150–154 salt bridge allowed the Arg 150 side chain to return to the receptor binding region. To confirm this prediction, we determined the structure of the apoE2 Ala 154 mutant 22,000  $M_r$  fragment by X-ray crystallography and compared it with a new and improved model of the structure of the apoE3 22,000  $M_r$  fragment, based on higher resolution data than were available in the previous model<sup>11</sup>. Data collection and merging statistics of the parallel data sets are given in Table 1. The overall features of the new apoE3 fragment model are very similar to the previous model<sup>11</sup>. The structure contains five  $\alpha$ -helices, four of which are arranged in an anti-parallel four-helix bundle (Fig. 3). The helices in the bundle are unusually elongat-

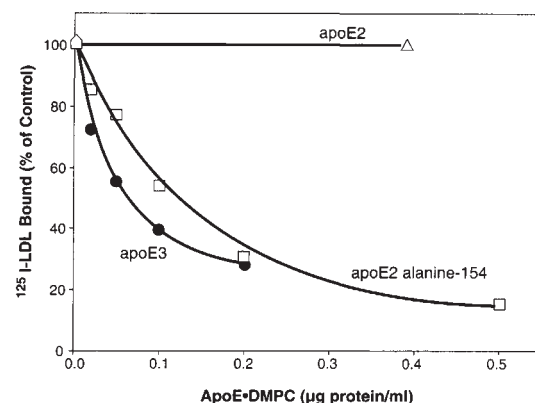
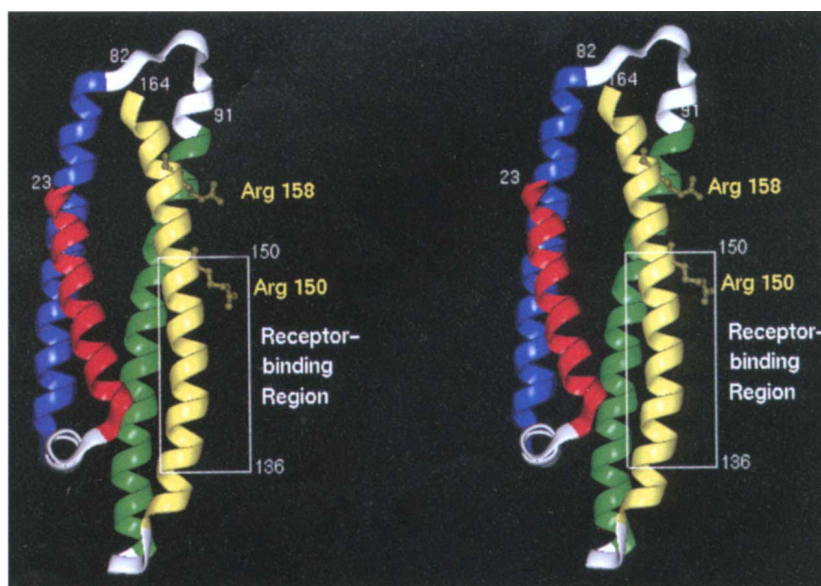


**Fig. 2** Comparison of the abilities of apoE3, apoE2 and apoE2 Ala 154 to compete with  $^{125}\text{I}$ -LDL receptors on normal human fibroblasts (see Methods). ApoE3 (●); ApoE2 (Δ); ApoE2 Ala 154 (□).

**Fig. 3** Ribbon model of the structure of the apoE3 22,000  $M_r$  fragment (residues 1–191). The model is based on 1.8 Å resolution data and begins at residue 23 and extends to residue 164. The beginnings and ends of the helices in the four-helix bundle are indicated: helix 1 (red) residues 23–43; helix 2 (blue) residues 53–81; helix 3 (green) residues 88–125; and helix 4 (yellow) residues 130–165. The loop between helices 2 and 3 and a portion of helix 3 (residues 82–91), which is undefined by electron density, are from the predicted loop in the previous apoE3 model<sup>19</sup>. The positions of Arg 158 and 150 are indicated and the receptor binding region (residues 136–150) is indicated by the boxed area.





ed. The backbone structure of apoE2 Ala 154 is essentially identical to the apoE3 structure. Within the four-helix bundles of both models, the electron density is clear and sharp. In the vicinity of the LDL receptor binding region (residues 136–150), the amino acid side chains are well defined. Despite slight conformational differences at atoms C $\gamma$  and C $\delta$ , both Arg 150 side chains point in similar directions, away from the site of residue 154 (Figs 4, 5) and into the receptor binding region. Clearly, the positions of the Arg 150 side chains in both apoE3 and apoE2 Ala 154 are similar to each other, but quite different from the position of this side chain in apoE2 (Fig. 1).

The importance of Arg 150 in receptor binding was suggested from previous mutagenesis studies<sup>7</sup>. Replacement of Arg 150 with Ala in apoE3 resulted in defective binding (24% of apoE3 binding activity). The present studies not only confirm the importance of Arg at this

position, but also demonstrate that the conformation of this side chain is critically important for normal receptor binding activity. In addition, these data prove the previous prediction that Arg 158 does not directly interact with the LDL receptor<sup>9</sup>, as nearly normal binding activity occurs with Cys at position 158 in the apoE2 Ala 154 mutant.

Formation and disruption of salt bridges in proteins as a result of mutations have been suggested to be critical in protein functions, including polymerase activity<sup>12</sup> and receptor recognition<sup>13</sup>; these changes can result in disease<sup>14</sup>. Disruption of a salt bridge in human immunodeficiency virus 1 reverse transcriptase between Asp 488 and Lys 465 by site-directed mutagenesis lowers its polymerase activity threefold<sup>12</sup>. In the case of transferrin, formation of a salt bridge between Arg 394 and Asp 392 in a naturally occurring mutant in which Arg replaces Gly 394 eliminates Asp 392 as a binding site for iron and reduces the affinity to receptors on phytohaemagglutinin-stimulated lymphocytes 10-fold<sup>13</sup>. Furthermore, any mutation in the visual pigment rhodopsin that disrupts a salt bridge between Lys 296 and Glu 113 activates opsin, causing congenital night blindness<sup>14</sup>. In contrast to the above examples, which involve either disruption or formation of salt bridges, the apoE2 mechanism is novel in that the defective binding results from the disruption of an existing salt bridge (Arg 158 and Asp 154) and formation of a new salt bridge (Asp 154 and Arg 150), which is responsible for the binding defect.

The binding of apoE2 to receptors can be highly variable: for example, the binding activity of apoE2 when complexed with dimyristoylphosphatidylcholine (DMPC)—forming discoidal lipoprotein particles—is invariably defective (<0.1% of apoE3 activity), while the binding activities of apoE2-containing spherical lipoprotein particles can vary from defective to near normal levels, depending on the lipid composition of the particles<sup>15</sup>. This variability in binding activities has been suggested to account for the fact that, while apoE2 is associated with type III hyperlipoproteinemia, homozygosity for apoE2 as well as additional genetic or environmental factors are required for expression of the phenotype (that is, expression is recessive and there is low penetrance of the phenotype)<sup>5</sup>.

We propose that the variability in receptor binding activity of apoE2-containing lipoproteins results from variability in the Arg 150 side-chain conformation (that is, whether the 154–150 salt bridge is formed or not), and that this variability is influenced by different lipid compositions or type of particles (for example, discoidal *versus* spherical). This is in contrast to a number of rare apoE mutants that occur within the receptor binding region that are associated with dominant expression of type III hyperlipoproteinemia<sup>5</sup>. In these cases, the receptor binding activity is invariably defective under all conditions of lipid association, and with these mutants there is a high penetrance of the phenotype, even in the heterozygous condition.

Predisposing factors for type III hyperlipoproteinemia such as obesity and a high-fat diet likely change the composition of apoE-containing lipoproteins<sup>15</sup>, modi-

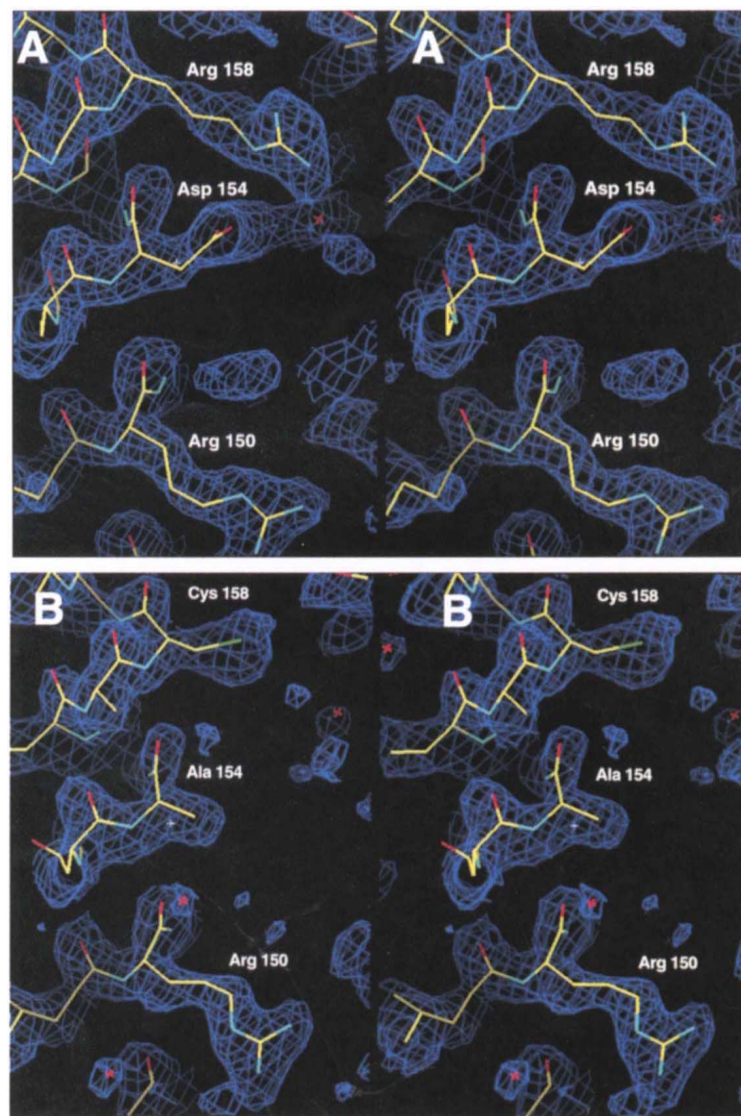


**Fig. 4** Stereo pair electron density maps (coefficients  $2F_o - F_c$ , contoured at the  $1\sigma$  level) in the vicinity of residue 150. *a*, ApoE3; *b*, ApoE2 Ala 154: x's denote positions of water molecules.

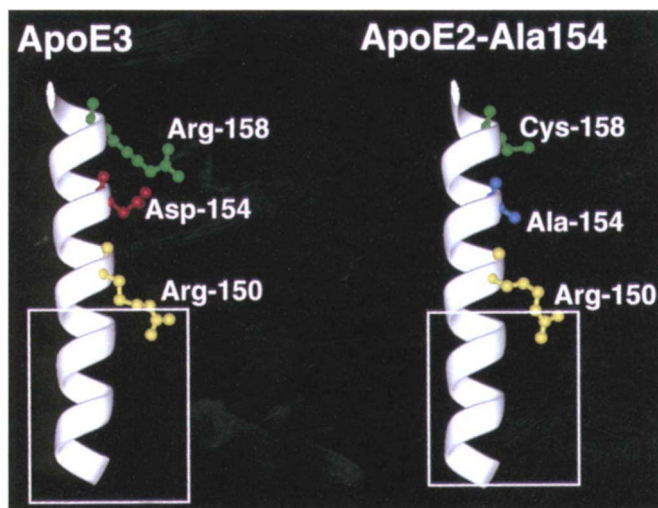


**Fig. 5** Ribbon representation of the  $\alpha$ -helical structure in the vicinity of the LDL receptor binding region of apoE3 and apoE2 Ala 154. The LDL receptor binding region is indicated by the boxed area. The position of Arg 150 is within the receptor binding region and is in an identical position as it is in apoE3. Model was prepared using Insight II (Biosym).

ifying the conformation of apoE such that the Arg 150–Asp 154 salt bridge is formed on most lipoprotein particles. In this defective binding form, all apoE-mediated clearance of lipoproteins would be delayed, resulting in hyperlipoproteinemia. In contrast, a low-fat, low-caloric diet and reduction in body weight may alter the lipid composition of lipoproteins such that significant amounts of the apoE2 are in a receptor-active conformation (that is, the Arg 150–Asp 154 bond is not formed). In this situation, apoE-mediated clearance of lipoproteins would be normal or near normal. It is important to note that subjects with type III hyperlipoproteinemia are particularly responsive to dietary treatment<sup>5</sup>. This scenario is consistent with the fact that in apoE2 homozygotes secondary factors are required for the development of type III hyperlipoproteinemia.

## Methods

**Expression and purification.** The glutathione S-transferase (GST) fusion expression vector pGEX3X<sup>16</sup> was used for expression of apoE mutants. The apoE2 Ala 154 mutant was created by the polymerase chain reaction as described previously<sup>17</sup>. Sequences of constructs were verified by double-stranded DNA sequencing. The expression was induced by addition of isopropyl  $\beta$ -D-thiogalactoside (IPTG) (Sigma). The expressed fusion protein was purified by glutathione-agarose affinity chromatography and cleaved with Factor Xa (Haematologic Technologies, Inc.) at a ratio of 200:1 (w/w, fusion protein:Factor Xa) at 0 °C overnight as described previously<sup>17</sup>. The apoE2 Ala 154 was purified by chromatography on a Sephacryl S-300 gel permeation column.

The apoE2 Ala-154 22,000 *M<sub>r</sub>* fragment was prepared by digestion of the intact variant with thrombin, as described<sup>6</sup>, and isolated on an HPLC DEAE ion-exchange column (21.5×150 mm, Bio-Rad), using a linear NaCl gradient. The apoE3 22,000 *M<sub>r</sub>* fragments were prepared using a T7 bacterial expression system<sup>18</sup>. After induction with IPTG, cells were harvested, resuspended in a 1/200 volume of cold sonication buffer (0.15 M NaCl, 20 mM Na<sub>2</sub>HPO<sub>4</sub>, pH 7.4, 25 mM EDTA, 1% aprotinin (Sigma), 0.1%  $\beta$ -mer-

captoethanol (Sigma), 2 mM PMSF (Sigma)), and lysed using a Branson Sonifier 450. After centrifugation to remove cellular debris, guanidine-HCl (ICN) was added to a final concentration of 7 M and the lysate was loaded onto a Sephacryl S-300 column (3 m×2.5 cm) and eluted with Tris-HCl buffer, pH 7.4, containing 4 M guanidine-HCl, 1 mM EDTA, and 0.1%  $\beta$ -mercaptoethanol at 1.0 ml/min. The apoE3 fragment was further purified by HPLC (Gilson) on a 21.5×150 mm DEAE column (Supelco).

**Crystallography.** Crystals were grown by vapour diffusion using the hanging drop method. Conditions were similar to those established previously for the apoE3 fragment obtained from plasma sources: 18–20% polyethylene glycol (PEG) 400 (Fluka), 20 mM sodium acetate (pH 5.8–6.0)<sup>11</sup>. The apoE3 22,000 *M<sub>r</sub>* fragment crystals were transferred to a modified reservoir solution containing 25% 2-methyl 2,4-pentanediol. They were mounted in a drop of this antifreeze solution in a fine glass loop, and placed in the cold stream of a modified Siemens LT-2 low-temperature device at 130 K. The apoE2 Ala 154 mutant crystals were mounted in a hair loop in a similar manner after a brief wash in a modified reservoir solution containing 30% PEG 400. Diffraction data to the resolution limit (1.8 Å for apoE3 and 2.0 Å for apoE2 Ala 154) were collected at 130 K using dual multiwire area detectors (Area Detector Systems Corp.) and graphite monochromated CuK $\alpha$  x-rays (Rigaku RU-200). Both crystals were orthorhombic, space group P2<sub>1</sub>2<sub>1</sub>2<sub>1</sub>, with *a*=40.70 Å, *b*=53.36 Å, *c*=84.51 Å and *a*=40.61 Å, *b*=53.67 Å, *c*=84.70 Å, respectively.

Starting coordinates for the apoE3 refinement were adapted from Protein Data Bank entry 1lpe, a 2.5 Å model of apoE3 determined by Wilson *et al.*<sup>11</sup>. Structure coordinates can be obtained from: khg@oedipus.llnl.gov, username: anonymous, password: e-mail address, cd pub/pdb\_files/apoE\_files, get apoE3.pdb, get apoE2.pdb. Unrealistic parts of the model were omitted. The starting point for the apoE2 Ala 154 refinement was a partially refined model of apoE3 in which residues 154 and 158 had been removed. Bond length and angle restraints imposed during refinement were those given by Engh and Huber<sup>19</sup>. Early stages of refinement were performed with both SHELXL-93<sup>20</sup> and X-PLOR<sup>21</sup> followed by model rebuilding in XtalView<sup>22</sup>. Positions for residues Cys 158 and Ala 154 in the apoE2 Ala 154 mutant and water molecules in both models were obtained from difference maps. Omit maps of randomly chosen regions and the *R<sub>free</sub>* statistic<sup>23</sup> were monitored to cross-check the results in real and reciprocal space respectively. Recognizable density in the N- and C-terminal regions and in a loop between residues 82–91 could not be found. At this stage, *R*-factors were 23.6% and 24.5% for apoE3 and apoE2 Ala 154 respectively. A holographic reconstruction of the electron density, made with the EDEN program<sup>24</sup> provided much improved phase estimates. The models were completely rebuilt using these phases, and absorption effects were corrected with XABS2<sup>25</sup>.

Further sophistication of the models (adding waters) was stopped when improvements indicated by *R<sub>free</sub>* were negligible (final values of *R<sub>free</sub>* were 25.9% and 27.0% for apoE3 and apoE2 Ala 154 respectively). Final refinements using SHELXL-93 gave *R*-factors of 20.9% for apoE3 against all data in the range 8.0–1.8 Å and 20.6% for apoE2 Ala 154 against all data between 8.0 Å and 2.0 Å. The apoE3 model contains residues 23–81 and 92–164 whereas the apoE2 Ala-154 model is truncated at glutamine 163. The missing residues, which constitute about 30% of the full 22,000 *M<sub>r</sub>* fragment are all located at one extreme of the four-helix bundle. We believe them to be completely disordered and thus indicate a likely cause of the rather high terminal *R*-values. The final models were checked with the PROCHECK



program<sup>26</sup>. Bond length and angle deviations from the Engh and Huber<sup>19</sup> ideal values were 0.011 Å, 0.010 Å, 2.0° and 2.0°, respectively for apoE3 and apoE2 Ala 154.

**Receptor binding assays.** Human apoE2 and apoE3 were isolated from the  $d > 1.006$  g ml<sup>-1</sup> lipoproteins, as described previously<sup>27</sup>. Human LDL were isolated from plasma of normal fasting subjects by sequential ultracentrifugation<sup>28</sup> and radiolabelled by the iodine monochloride method<sup>29</sup>. Various forms of apoE and dimyristoylphosphatidylcholine (DMPC) were mixed at a ratio of 1:3.75 (w/w,

protein:DMPC) and complexes were isolated by density gradient ultracentrifugation<sup>30</sup>. Normal human fibroblasts were plated at  $3.5 \times 10^4$  cells/dish one week before the experiment. On day 5, the cells were switched to a medium containing 10% lipoprotein-deficient serum. On day 7, the cells were incubated in at 4 °C of medium containing 2.0 µg ml<sup>-1</sup> of <sup>125</sup>I-LDL and various concentrations of apoE•DMPC. The competitive binding of apoE•DMPC against <sup>125</sup>I-LDL was determined as described previously<sup>30</sup>.

Received 17 April; accepted 25 June 1996.

## Acknowledgements

The authors thank H. Szöke for performing the EDEN calculations, K. Humphrey and S. White for manuscript preparation, J. Carroll and A. Corder for graphic arts, and G. Howard for editorial assistance. This work was supported by a National Institutes of Health Program Project Grant. The work described was carried out in part at the General Clinical Research Center, San Francisco General Hospital Medical Center, with support from a grant from the National Center for Research Resources, NIH. The work described was performed in part under the auspices of the Department of Energy at Lawrence Livermore National Laboratory.

1. Mahley, R.W. Apolipoprotein E: Cholesterol transport protein with expanding role in cell biology. *Science* **240**, 622–630 (1988).
2. Weisgraber, K.H. Apolipoprotein E: Structure–function relationships. *Adv. Prot. Chem.* **45**, 249–302 (1994).
3. Weisgraber, K.H., Rall, S.C., Jr. & Mahley, R.W. Human E apoprotein heterogeneity. Cysteine arginine interchanges in the amino acid sequence of the apo-E isoforms. *J. Biol. Chem.* **256**, 9077–9083 (1981).
4. Weisgraber, K.H., Innerarity, T.L. & Mahley, R. W. Abnormal lipoprotein receptor-binding activity of the human E apoprotein due to cysteine arginine interchange at a single site. *J. Biol. Chem.* **257**, 2518–2521 (1982).
5. Mahley, R.W. & Rall, S.C., Jr. In *The Metabolic and Molecular Bases of Inherited Disease* 7th ed (eds. Scriver, C.R., Beaudet, A.L., Sly, W.S. & Valle, D.) 1953–1980 (McGraw-Hill, New York, 1995).
6. Innerarity, T.L., Friedlander, E.J., Rall, S.C., Jr., Weisgraber, K.H. & Mahley, R.W. The receptor-binding domain of human apolipoprotein E. Binding of apolipoprotein E fragments. *J. Biol. Chem.* **258**, 12341–12347 (1983).
7. Lalazar, A. et al. Site-specific mutagenesis of human apolipoprotein E. Receptor binding activity of variants with single amino acid substitutions. *J. Biol. Chem.* **263**, 3542–3545 (1988).
8. Weisgraber, K.H. et al. The receptor-binding domain of human apolipoprotein E. Monoclonal antibody inhibition of binding. *J. Biol. Chem.* **258**, 12348–12354 (1983).
9. Innerarity, T.L., Weisgraber, K.H., Arnold, K.S., Rall, S.C., Jr. & Mahley, R.W. Normalization of receptor binding of apolipoprotein E2. Evidence for modulation of the binding site conformation. *J. Biol. Chem.* **259**, 7261–7267 (1984).
10. Wilson, C. et al. Salt bridge relay triggers defective LDL receptor binding by a mutant apolipoprotein. *Structure* **2**, 713–718 (1994).
11. Wilson, C., Wardell, M.R., Weisgraber, K.H., Mahley, R.W. & Agard, D.A. Three-dimensional structure of the LDL receptor-binding domain of human apolipoprotein E. *Science* **252**, 1817–1822 (1991).
12. Goobar-Larsson, L. et al. Disruption of a salt bridge between Asp 488 and Lys 465 in HIV-1 reverse transcriptase alters its proteolytic processing and polymerase activity. *Virology* **196**, 731–738 (1993).
13. Evans, R.W. et al. Characterization and structural analysis of a functional human serum transferrin variant and implications for receptor recognition. *Biochemistry* **33**, 12512–12520 (1994).
14. Rao, V.R., Cohen, G.B. & Oprian, D.D. Rhodopsin mutation G90D and a molecular mechanism for congenital night blindness. *Nature* **367**, 639–642 (1994).
15. Innerarity, T.L., Hui, D.Y., Bersot, T.P. & Mahley, R.W. Type III hyperlipoproteinemia: A focus on lipoprotein receptor-apolipoprotein E2 interactions. *Adv. Exp. Med. Biol.* **201**, 273–288 (1986).
16. Smith, D.B. & Johnson, K.S. Single-step purification of polypeptides expressed in *Escherichia coli* as fusions with glutathione S-transferase. *Gene* **67**, 31–40 (1988).
17. Dong, L.-M. et al. Human apolipoprotein E. Role of arginine 61 in mediating the lipoprotein preferences of the E3 and E4 isoforms. *J. Biol. Chem.* **269**, 22358–22365 (1994).
18. Studier, F.W. & Moffatt, B.A. Use of bacteriophage T7 RNA polymerase to direct selective high-level expression of cloned genes. *J. Mol. Biol.* **189**, 113–130 (1986).
19. Engh, R.A. & Huber, R. Accurate bond and angle parameters for X-ray protein structure refinement. *Acta Crystallogr.* **A47**, 392–400 (1991).
20. Sheldrick, G.M. SHELX-93 crystal structure refinement program. (1993).
21. Brünger, A. T. X-PLOR, Version 3.1. A System for X-ray Crystallography and NMR. (Yale University Press, New Haven, 1992).
22. McRee, D.E. *Practical Protein Crystallography*. (Academic Press, San Diego, 1993).
23. Brünger, A. T. Free R value: A novel statistical quantity for assessing the accuracy of crystal structures. *Nature* **355**, 472–475 (1992).
24. Somoza, J.R. et al. Holographic methods in X-ray crystallography. IV. A fast algorithm and its application to macromolecular crystallography. *Acta Crystallogr.* **A51**, 691–708 (1995).
25. Parkin, S., Moezzi, B. & Hope, H. XA852: An empirical absorption correction program. *J. Appl. Crystallogr.* **28**, 53–56 (1995).
26. Laskowski, R.A., MacArthur, M.W., Moss, D.S. & Thornton, J.M. PROCHECK: A program to check the stereochemical quality of protein structures. *J. Appl. Crystallogr.* **26**, 283–291 (1993).
27. Rall, S.C., Jr., Weisgraber, K.H. & Mahley, R.W. Isolation and characterization of apolipoprotein E. *Methods Enzymol.* **128**, 273–287 (1986).
28. Innerarity, T.L., Mahley, R.W., Weisgraber, K.H. & Bersot, T.P. Apoprotein (E-A-II) complex of human plasma lipoproteins. II. Receptor binding activity of a high density lipoprotein subfraction modulated by the apo(E-A-II) complex. *J. Biol. Chem.* **253**, 6289–6295 (1978).
29. Bilheimer, D.W., Eisenberg, S. & Levy, R.I. The metabolism of very low density lipoprotein proteins. I. Preliminary *in vitro* and *in vivo* observations. *Biochim. Biophys. Acta* **260**, 212–221 (1972).
30. Innerarity, T.L., Pitas, R.E. & Mahley, R.W. Binding of Arg rich (E) apoprotein after recombination with phospholipid vesicles to the low density lipoprotein receptors of fibroblasts. *J. Biol. Chem.* **254**, 4186–4190 (1979).